

## Ambient Reductive Amination of Levulinic Acid to Pyrrolidones over Pt Nanocatalysts on Porous TiO<sub>2</sub> Nanosheets

Chao Xie, Jinliang Song, Haoran Wu, Yue Hu, Huizhen Liu, Zhanrong Zhang, Pei Zhang, Bingfeng Chen, and Buxing Han

*J. Am. Chem. Soc.*, **Just Accepted Manuscript** • DOI: 10.1021/jacs.8b13024 • Publication Date (Web): 10 Feb 2019

Downloaded from <http://pubs.acs.org> on February 10, 2019

### Just Accepted

“Just Accepted” manuscripts have been peer-reviewed and accepted for publication. They are posted online prior to technical editing, formatting for publication and author proofing. The American Chemical Society provides “Just Accepted” as a service to the research community to expedite the dissemination of scientific material as soon as possible after acceptance. “Just Accepted” manuscripts appear in full in PDF format accompanied by an HTML abstract. “Just Accepted” manuscripts have been fully peer reviewed, but should not be considered the official version of record. They are citable by the Digital Object Identifier (DOI®). “Just Accepted” is an optional service offered to authors. Therefore, the “Just Accepted” Web site may not include all articles that will be published in the journal. After a manuscript is technically edited and formatted, it will be removed from the “Just Accepted” Web site and published as an ASAP article. Note that technical editing may introduce minor changes to the manuscript text and/or graphics which could affect content, and all legal disclaimers and ethical guidelines that apply to the journal pertain. ACS cannot be held responsible for errors or consequences arising from the use of information contained in these “Just Accepted” manuscripts.



# Ambient Reductive Amination of Levulinic Acid to Pyrrolidones over Pt Nanocatalysts on Porous TiO<sub>2</sub> Nanosheets

Chao Xie,<sup>†,‡</sup> Jinliang Song,<sup>\*,†</sup> Haoran Wu,<sup>†,‡</sup> Yue Hu,<sup>†,‡</sup> Huizhen Liu,<sup>†,‡</sup> Zhanrong Zhang,<sup>†</sup> Pei Zhang,<sup>†</sup> Bingfeng Chen,<sup>†</sup> and Buxing Han<sup>\*,†,‡</sup>

<sup>†</sup>Beijing National Laboratory for Molecular Science, CAS Key Laboratory of Colloid and Interface and Thermodynamics, CAS Research/Education Center for Excellence in Molecular Sciences, Institute of Chemistry, Chinese Academy of Sciences, Beijing 100190, China.

<sup>‡</sup>School of Chemistry and Chemical Engineering, University of Chinese Academy of Sciences, Beijing 100049, China.

## Supporting Information Placeholder

**ABSTRACT:** Construction of *N*-substituted pyrrolidones from biomass-derived levulinic acid (LA) *via* reductive amination is a highly attractive route for biomass valorization. However, realizing this transformation using H<sub>2</sub> as the hydrogen source under mild conditions is still very challenging. Herein, we designed porous TiO<sub>2</sub> nanosheets supported Pt nanoparticles (Pt/P-TiO<sub>2</sub>) as the heterogeneous catalyst. The prepared Pt/P-TiO<sub>2</sub> was highly efficient for reductive amination of LA to produce various *N*-substituted pyrrolidones (34 examples) at ambient temperature and H<sub>2</sub> pressure. Meanwhile, Pt/P-TiO<sub>2</sub> showed good applicability for reductive amination of levulinic esters, 4-acetylbutyric acid, 2-acetylbenzoic acid and 2-carboxybenzaldehyde. Systematic studies indicated that the strong acidity of P-TiO<sub>2</sub> and the lower electron density of the Pt sites as well as the porous structure resulted in the excellent activity of Pt/P-TiO<sub>2</sub>.

## INTRODUCTION

In the pursuit of a sustainable future, biomass has been recognized as a renewable alternative for fossil resources to produce various high-valued chemicals, and diverse strategies have been established for biomass transformation.<sup>1</sup> In this context, levulinic acid, a valuable platform chemical from lignocellulosic biomass, has attracted much interest because it can be upgraded into some valuable chemicals,<sup>2</sup> in which *N*-alkyl-5-methyl-2-pyrrolidones, produced through reductive amination of LA,<sup>3</sup> are significantly attractive to be used as industrial solvents, dispersants, and surfactants.<sup>4</sup>

Generally, LA can be converted into *N*-alkyl-5-methyl-2-pyrrolidones *via* reductive amination by employing formic acid or organosilanes as the hydrogen sources.<sup>4b, 4c, 5</sup> However, some drawbacks hindered the large-scale application of these two hydrogen sources, such as the corrosiveness of formic acid, the high price and excess usage of organosilanes, and harsh reaction conditions, *etc.* Compared with formic acid and organosilanes, H<sub>2</sub> is the more desired hydrogen source from economic and industrial viewpoints. To dates, several catalysts have been explored for reductive amination of LA using H<sub>2</sub> as hydrogen source, including supported metal

catalysts (*i.e.*, Pt, Pd, Rh, Ru, Co, Ni),<sup>3a, 3b, 4b, 6</sup> and homogeneous metal (Ir, Ru) complex.<sup>5b, 7</sup> However, these catalysts usually required either high H<sub>2</sub> pressure (>3 MPa) and temperature (>100 °C) or only provided low to moderate product yields. Therefore, it is highly desired to develop efficient heterogeneous catalysts for reductive amination of LA to *N*-alkyl-5-methyl-2-pyrrolidones with H<sub>2</sub> at ambient conditions.

As well-known, the catalytic activity of supported metal catalysts can be significantly enhanced by utilizing functional support materials.<sup>8</sup> There is great potential to prepare efficient heterogeneous catalysts for reductive amination of LA by designing functional support materials. Herein, we prepared porous TiO<sub>2</sub> nanosheets (denoted as P-TiO<sub>2</sub>) as a functional support for Pt nanoparticles (Pt NPs). P-TiO<sub>2</sub> supported Pt NPs (denoted as Pt/P-TiO<sub>2</sub>) showed excellent performance for the reductive amination of LA with a range of primary amines even at ambient temperature and H<sub>2</sub> pressure. To the best of our knowledge, this is the first work to realize this kind of reactions at ambient conditions.

## RESULTS AND DISCUSSION

**Preparation and Characterization of the Pt/P-TiO<sub>2</sub>.** The P-TiO<sub>2</sub> nanosheets was prepared through a ball milling route using KNO<sub>3</sub> as the hard template, and Pt NPs were supported on the prepared P-TiO<sub>2</sub> to form Pt/P-TiO<sub>2</sub> with NaBH<sub>4</sub> as the reducing agent. Detail preparation processes for P-TiO<sub>2</sub> and Pt/P-TiO<sub>2</sub> was described in the Experimental Section. The morphology of the synthesized P-TiO<sub>2</sub> and Pt/P-TiO<sub>2</sub> was firstly examined by TEM and SEM (Figure 1a-d). TEM images indicated that P-TiO<sub>2</sub> had a porous nanosheet structure (Figure 1a-b), which was retained after supporting Pt NPs (Figure 1c). In Pt/P-TiO<sub>2</sub>, Pt NPs had an average size of 2.4 nm (Figure S1). High resolution TEM (HR-TEM) image showed that Pt NPs on the P-TiO<sub>2</sub> had an interplanar distance of 0.19 nm, corresponding to the distinct lattice fringe of Pt (200) surface. N<sub>2</sub> adsorption-desorption isotherm indicated that P-TiO<sub>2</sub> had a BET surface area of about 259.8 m<sup>2</sup>/g (Figure 1e), and meanwhile, the pore distribution confirmed the existence of micropores in P-TiO<sub>2</sub>, which was consistent with the TEM

result (Figure 1a). The XRD patterns of P-TiO<sub>2</sub> and Pt/P-TiO<sub>2</sub> suggested that these two materials had low crystallinity (Figure 1f), and no peak for Pt species was found in the pattern for Pt/P-TiO<sub>2</sub>, indicating no aggregation of Pt NPs. Additionally, the content of Pt in Pt/P-TiO<sub>2</sub> was 1.98 wt% determined by ICP-AES (VISTA-MPX), and the Pt dispersion in Pt/P-TiO<sub>2</sub> was 21% determined by CO-pulse titration (Table S1).

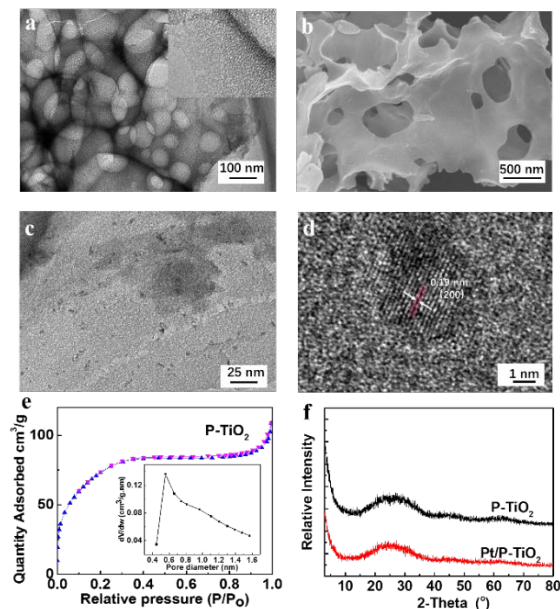


**Figure 1.** Characterization of the obtained P-TiO<sub>2</sub> and Pt/P-TiO<sub>2</sub>. TEM (a) and SEM (b) images of P-TiO<sub>2</sub>, TEM (c) and HR-TEM (d) images of Pt/P-TiO<sub>2</sub>. N<sub>2</sub> adsorption-desorption isotherms (e) of P-TiO<sub>2</sub> (Insert e: the distribution of micropore), and XRD patterns (f) of P-TiO<sub>2</sub> and Pt/P-TiO<sub>2</sub>.

**Activity of Various Catalysts.** As a common used catalyst, supported Pt showed good performance for reductive amination of LA under high H<sub>2</sub> pressure and temperature.<sup>3a, 3b, 6a, 6b</sup> Therefore, we initially evaluate the catalytic activity of several Pt-based catalysts with similar Pt dispersion and crystal size of Pt particles (Table S1) at ambient conditions employing reductive amination of LA with *n*-octylamine as a model reaction (Table 1). No target product was formed without any catalysts (Table 1, entry 1). Commercial Pt/C showed very low activity (Table 1, entries 2). To our delight, the Pt/P-TiO<sub>2</sub> prepared in this work could catalyze the reaction very efficiently with the highest TOF (Table 1, entry 3). Furthermore, the Pt particles supported on commercial TiO<sub>2</sub> and P25 (Pt/TiO<sub>2</sub> and Pt/P25) provided much lower activity (Table 1, entries 4 and 5) than Pt/P-TiO<sub>2</sub>, suggesting the intrinsic advantage of the prepared P-TiO<sub>2</sub>. In addition, the reactants could be fully converted with a product yield of 97% over Pt/P-TiO<sub>2</sub> in 3 h (Table 1, entry 6, and Figure S2). Moreover, Pt/P-TiO<sub>2</sub> showed much higher activity than the reported catalysts (Table S2). These results indicated Pt/P-TiO<sub>2</sub> was a superior catalyst for reductive amination of LA, and the reason for the excellent performance will be discussed below. In another aspect, some control experiments were conducted to examine the reaction efficiency under solvent-free conditions. Without using solvents, the yield of the desired product over the synthesized Pt/P-TiO<sub>2</sub> and the conventional Pt/TiO<sub>2</sub> were 7% and 2%, respectively (Table 1, entries 7 and 8). The difference in activity of the two catalysts

under solvent-free conditions was not significant because the high viscosity of the reaction system under solvent-free conditions, which was resulted from the strong interaction between the carboxyl group in LA and the amino group in *n*-octylamine, was an important factor for the reaction efficiency, especially at room temperature. Therefore, it is necessary to use the solvent in the reaction using LA as the reactant for high efficiency. Moreover, the influence of different solvents was examined for the reductive amination of LA with *n*-octylamine (Table S3). The yield of the desired product was very low in *n*-hexane (Table S3, entry 1) because the condensation of C=O in LA and NH<sub>2</sub> in *n*-octylamine was sluggish,<sup>9</sup> significantly lowering the total reaction rate. The aprotic polar solvents (*i.e.*, DMF, THF, 1,4-dioxane, and acetonitrile) were also unbeneficial for the reaction (Table S3, entries 2-5), which resulted from the occupation of the catalytic active sites on the Pt/P-TiO<sub>2</sub> by the solvent molecules due to their strong adsorption.<sup>9,10,3d</sup> In contrast, good results could be achieved in protic polar solvents, *i.e.*, methanol, ethanol, and isopropanol (Table S3, entries 6-8) because the protic polar solvents could accelerate both the condensation of C=O and NH<sub>2</sub> and the subsequent cyclization<sup>9</sup> (See the following mechanism section), resulting in higher reaction rate. Due to the best result in methanol (Table S3, entry 6), it was selected as the solvent. Additionally, the synthesized Pt/P-TiO<sub>2</sub> showed much higher activity than conventional Pt/TiO<sub>2</sub> when using methyl levulinate as the substrate under solvent-free conditions (Table 1, entries 9 and 10) because the interaction of ester group in methyl levulinate and the amino group in *n*-octylamine is relatively weak and the viscosity of the reaction system was relatively low. The results indicated that the synthesized Pt/P-TiO<sub>2</sub> was also more active than Pt/TiO<sub>2</sub> in solvent-free reaction system of low viscosity.

**Table 1.** Reductive amination of LA with *n*-octylamine over different catalysts.<sup>a</sup>

Entry	Catalyst	Yield (%)	TOF (h <sup>-1</sup> ) <sup>b</sup>
1	-	0	--
2	Pt/C	4	40 (222)
3	Pt/P-TiO <sub>2</sub>	61	610 (2905)
4	Pt/TiO <sub>2</sub>	14	140 (875)
5	Pt/P25	16	160 (941)
6 <sup>c</sup>	Pt/P-TiO <sub>2</sub>	97	323 (1538)
7 <sup>d</sup>	Pt/P-TiO <sub>2</sub>	7	70 (333)
8 <sup>d</sup>	Pt/TiO <sub>2</sub>	2	20 (125)
9 <sup>e</sup>	Pt/P-TiO <sub>2</sub>	58	193 (919)
10 <sup>e</sup>	Pt/TiO <sub>2</sub>	10	33 (206)

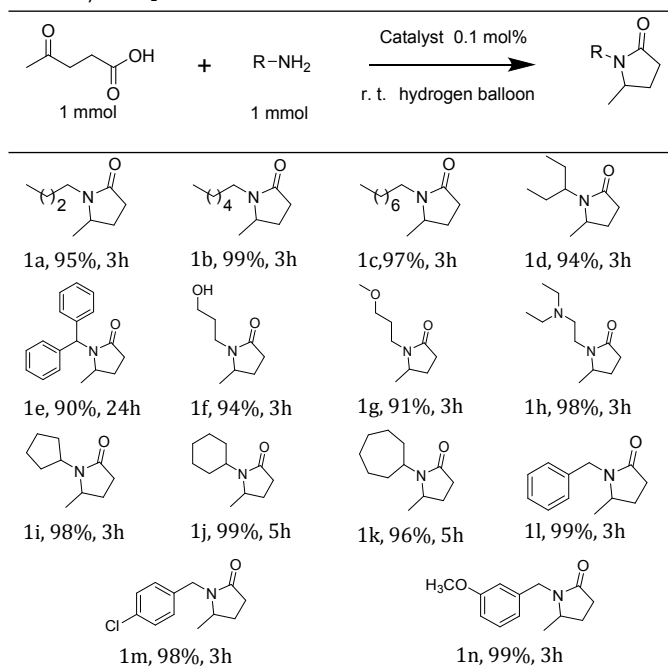
<sup>a</sup>Reaction conditions: LA, 1 mmol; *n*-octylamine, 1 mmol; catalyst, 0.1 mol% Pt; methanol, 2 ml; time, 1 h; temperature, r.t.; H<sub>2</sub> pressure, hydrogen balloon. <sup>b</sup>TOF = mol of product/mol of Pt×h<sup>-1</sup>, and values in parentheses were the TOF calculated based on Pt dispersion. <sup>c</sup>The reaction time was 3 h. <sup>d</sup>The reaction was conducted under solvent-free conditions with a reaction time of 1 h. <sup>e</sup>The reaction was conducted under solvent-free conditions using methyl levulinate and *n*-octylamine as reactants with a reaction time of 3 h.

**Reusability of the Prepared Pt/P-TiO<sub>2</sub>.** The heterogeneous nature of Pt/P-TiO<sub>2</sub> was evaluated by removing the catalyst after the reaction was conducted for 1 h, and then the reaction was continued for 4 h without solid catalyst. The product yield

was not further increased without Pt/P-TiO<sub>2</sub> (Figure S3a), indicating no leaching of active species to the reaction mixture. Meanwhile, the concentrations of Pt and Ti in the reaction solution were below detection limit of ICP-AES, further confirming the negligible leaching of Pt and Ti species and the heterogeneous nature of Pt/P-TiO<sub>2</sub>. Furthermore, the Pt/P-TiO<sub>2</sub> could be recycled several times without significant decrease in activity. The observed yield decreased slightly after 4 recycles, which could be attributed to the catalyst loss in the recovery process (Figure S3b). After the fourth run, 8 mg Pt/P-TiO<sub>2</sub> (80% original amount) was recovered. Therefore, in the fifth run, the amount of reactants was decreased based on the recovered catalyst and the yield was then restored. The recovered Pt/P-TiO<sub>2</sub> was characterized by TEM and XPS (Figure S4), and no considerable change was found. The above results indicate the high stability of Pt/P-TiO<sub>2</sub> in the reaction systems.

**Scope of the Substrates.** Delighted by the excellent performance of Pt/P-TiO<sub>2</sub> for reductive amination of LA with *n*-octylamine, the reactivity of various primary amines was subsequently investigated. Over Pt/P-TiO<sub>2</sub>, aliphatic amines could be efficiently converted into the corresponding *N*-alkyl-5-methyl-2-pyrrolidones with excellent yields (Table 2). Different from commonly reported results,<sup>5b</sup> the chain length of the aliphatic amines showed no obvious impact on the reactivity (Table 2, 1a-c) in our catalytic system. Meanwhile, Pt/P-TiO<sub>2</sub> could also efficiently catalyze reductive amination of LA with the aliphatic amines with branched chain (Table 2, 1d and 1e) and various functional groups (Table 2, 1f-h), cyclic amines (Table 2, 1i-k), and benzylic amines (Table 2, 1l-n).

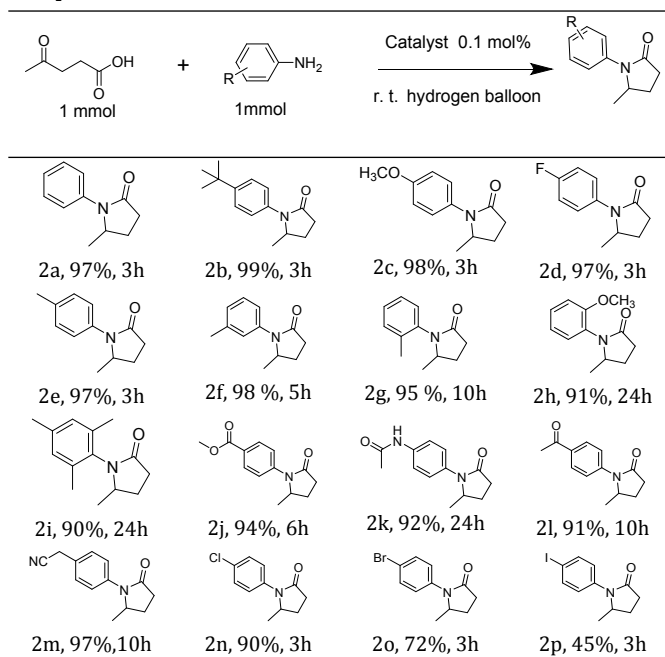
**Table 2.** Reductive amination of LA with various aliphatic amines over Pt/P-TiO<sub>2</sub>.



Furthermore, Pt/P-TiO<sub>2</sub> was also suitable for the reductive amination of LA with anilines (Table 3), and most of the examined anilines gave good yields (>90%) of corresponding pyrrolidones at ambient conditions. The

primary anilines with different substituted groups, including methyl, tertiary butyl, methoxy, and halogen, could be converted efficiently, affording the corresponding products in high yields (Table 3, 2a-e). Meanwhile, the reactivity of the methyl-substituted anilines followed the order: *p*-methyl aniline > *m*-methyl aniline > *o*-methyl aniline (Table 3, 2e-g) caused by the different steric effect. In addition, *o*-methoxyaniline and 2,4,6-trimethylaniline needed longer reaction time (24 h) to provide good yields due to the strong steric effect of the substituted groups (Table 3, 2h and 2i). Furthermore, the substrates with reduction-sensitive substituents were examined to study the applicability of the synthesized Pt/P-TiO<sub>2</sub>. High yields (>90%) of the desired products could be achieved when 4-aminobenzonitrile (2j), 4-aminoacetophenone (2k), 4-aminoacetanilide (2l) and methyl 4-aminobenzoate (2m) were used as the reactants. For halogen (Cl, Br, I)-substituted substrates (2n-p), the dehalogenation reaction with different extent occurred owing to the high activity of the synthesized Pt/P-TiO<sub>2</sub>, and the yields of the desired halogen-substituted products were 91%, 72% and 45% for 4-chloroaniline (2n), 4-bromoaniline (2o) and 4-iodoaniline (2p), respectively. However, the desired products (1-(4-ethynylphenyl)-5-methylpyrrolidin-2-one, and 1-(4-vinylphenyl)-5-methylpyrrolidin-2-one) were not obtained using 4-ethynylaniline and 4-vinylaniline as the substrates because the high activity of Pt/P-TiO<sub>2</sub> resulted in the complete hydrogenation of the ethynyl and vinyl groups to generate 1-(4-ethylphenyl)-5-methylpyrrolidin-2-one. Therefore, balancing the catalytic activity and the product selectivity was very important for the substrates with reduction-sensitive substituents.

**Table 3.** Reductive amination of LA with various anilines over Pt/P-TiO<sub>2</sub>.



Except for LA, Pt/P-TiO<sub>2</sub> could be employed to efficiently catalyze reductive amination of other substrates with the similar structure to LA at ambient conditions (Table 4). Various levulinic esters, a class of chemicals derived from carbohydrates in alcohols, could also be converted with *n*-octylamine to form *N*-octyl-5-methyl-2-pyrrolidones.

Compared with LA, levulinic esters showed relative lower reactivity, and longer reaction time (10 to 24 h) was needed to reach high product yields (Table 4, entries 1-4). The reactivity of levulinic esters followed the order: methyl levulinate > ethyl levulinate > butyl levulinate owing to the different steric hindrance effect. Meanwhile, Pt/P-TiO<sub>2</sub> could be further expanded to catalyze the reductive amination of 4-acetylbutyric acid to produce *N*-alkyl-2-piperidinones, which are another class of important heterocycle compounds. Taking *n*-octylamine as an example, *N*-octyl-2-piperidinone could be obtained from 4-acetylbutyric acid with a yield of 97% over Pt/P-TiO<sub>2</sub> (Table 4, entry 5). Furthermore, Pt/P-TiO<sub>2</sub> was applicable for reductive amination of 2-acetylbenzoic acid and 2-carboxybenzaldehyde to generate the corresponding *N*-arylisoindolinones with *n*-octylamine, and the product yields could reach 95% and 96%, respectively (Table 4, entries 6-7). In another aspect, the NH-free pyrrolidone was also an attractive compound. The synthesized Pt/P-TiO<sub>2</sub> was used to catalyze the reductive amination of LA using 25 wt% aqueous ammonia as the amine source (Table 4, entry 8). To our delight, a 85% yield of the corresponding NH-free pyrrolidone was successfully generated with a reaction time of 72 h under ambient conditions. Additionally, when using NH<sub>3</sub> (gas) as the amine source, the NH-free pyrrolidone could also be generated with a yield of 89% over the synthesized Pt/P-TiO<sub>2</sub> at room temperature (Table 4, entry 9). These results further indicated the extensive applicability and high activity of the synthesized Pt/P-TiO<sub>2</sub>.

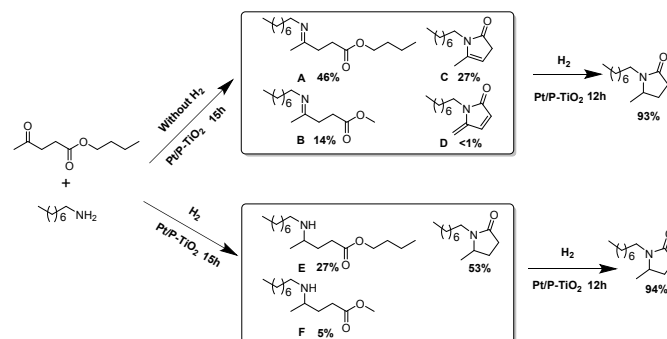
**Table 4.** Reductive amination of other substrates with *n*-octylamine over Pt/P-TiO<sub>2</sub>.<sup>a</sup>

Entry	Substrate	Product	Time (h)	Yield (%)
1			3	97
2			10	94
3			10	93
4			24	92
5			3	97
6			24	95
7			5	96
8 <sup>b</sup>			72	85
9 <sup>c</sup>			72	89

<sup>a</sup>Reaction conditions: substrate, 1 mmol; *n*-octylamine, 1 mmol; Pt/P-TiO<sub>2</sub>, 0.1 mol% Pt; methanol, 2 mL; r.t.; hydrogen balloon. <sup>b</sup>Reaction conditions: LA, 1 mmol; 25 wt% aqueous ammonia, 500  $\mu$ l; Pt/P-TiO<sub>2</sub>, 0.1 mol% Pt; methanol, 2 mL; r.t.; hydrogen balloon. <sup>c</sup>Reaction

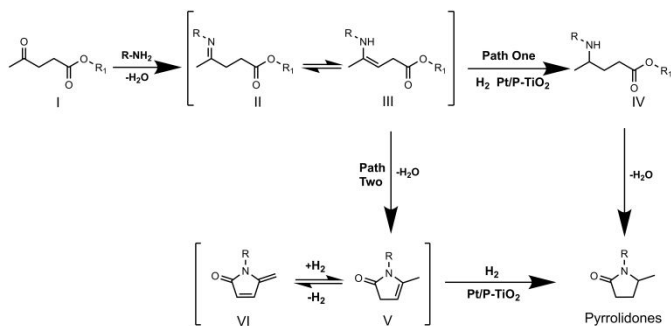
conditions: LA, 1 mmol; NH<sub>3</sub> (gas), 0.5 MPa; H<sub>2</sub>, 1.5 MPa; Pt/P-TiO<sub>2</sub>, 0.1 mol% Pt; methanol, 2 mL; r.t.

**Mechanism Discussion.** To get some evidences to study the reaction mechanism for the reductive amination of LA, some control experiments were conducted using butyl levulinate as the reactant (Scheme 1) because of the steric hindrance effect of butyl in butyl levulinate (Table 4, entry 4) was beneficial for obtaining the reaction intermediates, and the reaction process was monitored by GC-MS method (Figure S5-6). As reported,<sup>3b,3d,3e,6c</sup> the amine could react with ketone to form imine. In the absence of H<sub>2</sub>, the relative imines (A and B, B was generated from the transesterification of A with the solvent methanol) could be easily detected. Meanwhile, the cyclization products (C and D in Scheme 1, and D was the oxidative product of C)<sup>1c</sup> from isomer (enamine) of imine were determined by GC-MS (Figure S5), and C and D could also be easily detected when using LA as the reactant no matter with or without H<sub>2</sub> (Figure S7-8), indicating the cyclization of the enamine could be a possible pathway (Path Two in Scheme 2) for the studied reductive amination to synthesize pyrrolidines. In another aspect, when the H<sub>2</sub> was giving, the desired pyrrolidine, E and F (from the hydrogenation of the corresponding imines) became the main products (Scheme 1), and the corresponding intermediate F (Figure S9, NMR data) could be conveniently separated in a control experiment using butyl levulinate and aniline as the reactants. With a prolonged reaction time, both E and F could be further converted into the desired pyrrolidine. These results showed that the imine or enamine intermediate could be hydrogenated to the saturated intermediate and further cyclized into the desired pyrrolidone, confirming the occurrence of Path One in Scheme 2.



**Scheme 1.** Control experiments of reductive amination of butyl levulinate with *n*-octylamine.

On the basis of the above experimental results and previous reports,<sup>3c,4c,5a</sup> a possible mechanism for the reductive amination of LA and its esters to pyrrolidinones over Pt/P-TiO<sub>2</sub> was proposed (Scheme 2). Initially, the corresponding imine II was easily generated through the condensation reaction of the carbonyl groups in LA and its esters with the amino group in the amines.<sup>3b,3c,6c,5b,5c</sup> Subsequently, two reaction pathways were proceeded to form the desired pyrrolidone. In one pathway (Path One), the imine II was hydrogenated to amino group over the Pt sites, and then the corresponding *N*-substituted pyrrolidone was formed through the intramolecular cyclization of IV catalyzed by the acidic sites in the Pt/P-TiO<sub>2</sub>.<sup>3b, 6c</sup> In another pathway (Path Two), intermediates V and VI were firstly formed from the cyclization of the isomer of II (III). After hydrogenated on Pt sites, the two intermediates V and VI were converted to generate the desired pyrrolidone.<sup>3c</sup>



**Scheme 2.** A plausible mechanism for the reductive amination of LA and its esters to pyrrolidones over the prepared Pt/P-TiO<sub>2</sub>.

### Reasons for the High Activity of the Synthesized Pt/P-TiO<sub>2</sub>.

To investigate the reason for the excellent performance of the synthesized Pt/P-TiO<sub>2</sub> for the reductive amination of LA and its esters, the influence of reaction temperature on the catalytic performance of different catalysts (*i.e.*, the synthesized Pt/P-TiO<sub>2</sub>, conventional Pt/TiO<sub>2</sub>, and Pt/C) was examined to obtain the apparent activation energy ( $E_a$ ) via the Arrhenius equation.<sup>11</sup> The  $E_a$  of the reaction were calculated from the slope of  $-\ln(\text{TOF})$  versus  $1/T$  plots, and the results are presented in Figure 2a. The  $E_a$  of the catalytic systems promoted by different catalysts decreased in the order: the synthesized Pt/P-TiO<sub>2</sub> (30 kJ/mol) < conventional Pt/TiO<sub>2</sub> (84 kJ/mol) < Pt/C (89 kJ/mol), indicating the much stronger ability of the synthesized Pt/P-TiO<sub>2</sub> to reduce the  $E_a$  of the reaction than conventional Pt/TiO<sub>2</sub> and Pt/C, and thus achieved the highest catalytic activity. These results were consistent with the catalytic results shown in Table 1.

Generally, both the condensation of carbonyl groups and amino groups to form intermediate II (Scheme 2) and the cyclization of intermediates III and IV (Scheme 2) could be enhanced by the acidity of the catalyst. Therefore, the acidity of the synthesized Pt/P-TiO<sub>2</sub> and conventional Pt/TiO<sub>2</sub> was evaluated by different techniques in this work. NH<sub>3</sub>-TPD examination (Figure 2b) clearly showed the stronger acidity of P-TiO<sub>2</sub> than the conventional TiO<sub>2</sub>. Meanwhile, the higher binding energy values of Ti 2p in P-TiO<sub>2</sub> indicated the higher positive charge on Ti atoms in the P-TiO<sub>2</sub> than in conventional TiO<sub>2</sub> (Figure 2c), which resulted in stronger acidity.<sup>12</sup> To exclude the effect of residual KNO<sub>3</sub> on the acidity of P-TiO<sub>2</sub>, the acidity of the mixture of commercial TiO<sub>2</sub> (1 g) and KNO<sub>3</sub> (20 mg) was also determined by NH<sub>3</sub>-TPD (Figure 2b). No difference was found for the acidity of pure TiO<sub>2</sub> and the mixture when the NH<sub>3</sub> desorption temperature was below 450 °C, while the peak observed at 500 °C for both P-TiO<sub>2</sub> and the mixture resulted from the generated gases from KNO<sub>3</sub> decomposition rather than the acidity of the materials. In another aspect, the addition of KNO<sub>3</sub> showed no effect on the catalytic activity of Pt/P25 and Pt/TiO<sub>2</sub> (Table S4, entries 1-4). These control experiments suggested that the residual KNO<sub>3</sub> did not affect the acidity of P-TiO<sub>2</sub>. The higher acidity of the prepared P-TiO<sub>2</sub> may be attributed to that more acidic sites were exposed due to its unique structure (porous, and nanosheet). Furthermore, *in situ* acetone-DRIFT (DRIFT=diffuse reflectance infrared Fourier transform) spectra of P-TiO<sub>2</sub>, TiO<sub>2</sub>, Pt/P-TiO<sub>2</sub> and Pt/TiO<sub>2</sub> were conducted to examine the interaction between the carbonyl groups and the acidic sites on the catalysts (Figure 2d). The spectra in Figure 2d showed that the C=O stretching band of the adsorbed acetone shifted to lower wavenumber on the Pt/P-

TiO<sub>2</sub> and P-TiO<sub>2</sub> than those on Pt/TiO<sub>2</sub> and TiO<sub>2</sub>, indicating the stronger interaction of the carbonyl groups with the acidic sites of Pt/P-TiO<sub>2</sub> and P-TiO<sub>2</sub> than that of conventional Pt/TiO<sub>2</sub> and TiO<sub>2</sub>.<sup>3b,6c</sup> These results indicated that the stronger acidity of Pt/P-TiO<sub>2</sub> and the stronger interaction of the corresponding groups with the catalytic sites were beneficial for the condensation of carbonyl groups and amino groups and the corresponding cyclization (Scheme 2),<sup>13</sup> and thus leading to the high activity of the synthesized Pt/P-TiO<sub>2</sub> for the reductive amination of LA.

*In situ* CO-DRIFT measurements were performed to determine the electronic property of the supported Pt surface. As shown in Figure 2e, the band for CO adsorbed on metallic Pt (CO-Pt<sup>0</sup>) in the synthesized Pt/P-TiO<sub>2</sub> was observed at 2093 cm<sup>-1</sup>, which showed a blue-shift compared with the band (2079 cm<sup>-1</sup>) for CO adsorbed on metallic Pt (CO-Pt<sup>0</sup>) in conventional Pt/TiO<sub>2</sub>. The blue-shift of CO adsorption band indicated that the electron-donating capability of Pt in the Pt/P-TiO<sub>2</sub> was weaker than that in the conventional Pt/TiO<sub>2</sub> because the P-TiO<sub>2</sub> with higher acidity (Figure 2b) had higher ability to decrease the electron density of Pt particles than conventional TiO<sub>2</sub>.<sup>7b,14</sup> It has been reported that lower electron density of the catalytic sites (Pt particles in our systems) was beneficial for the desorption of the products and reactants, and thus resulted in higher catalytic activity.<sup>7b,15</sup> In our reaction system, both the reactant (amines) and the product (pyrrolidones) were nitrogen-containing compounds, and they could generate strong interaction with the Pt active sites, which could decrease the reaction rate due to the occupation and even poison of the active sites.<sup>16</sup> Therefore, the lower electron density of Pt in the synthesized Pt/P-TiO<sub>2</sub> probably resulted in a higher desorption rate of the used amines and the generated pyrrolidones from the active sites owing to their weaker interaction, and thus Pt/P-TiO<sub>2</sub> showed higher activity for the reductive amination of LA than the conventional Pt/TiO<sub>2</sub>. Furthermore, some control experiments using 5-methylpyrrolidin-2-one as an additive were conducted to show the different interaction ability of pyrrolidone with the active sites on the used Pt-based catalysts (Table S4). It was found that by the pre-addition of 5-methylpyrrolidin-2-one, the activity of Pt/TiO<sub>2</sub> and Pt/P25 decreased (Table S4, entries 7-8 vs. 3-4), while Pt/P-TiO<sub>2</sub> was not affected. (Table S4, entry 6 vs. 5). These results implied the weaker interaction ability of pyrrolidone with the active sites on Pt/P-TiO<sub>2</sub> owing to the lower electron density of Pt sites, resulting in a higher desorption rate of the generated pyrrolidone from Pt/P-TiO<sub>2</sub> to enhance the reductive amination of LA. The discussions above indicated that the lower electron density of Pt sites could improve the desorption of the generated pyrrolidone, which was an important parameter to affect the reaction rate.

Additionally, from the results of N<sub>2</sub> adsorption-desorption (Figure 2f), the prepared P-TiO<sub>2</sub> showed a high BET surface area (259.8 m<sup>2</sup>/g) due to its porous structure (Figure 1a), while the BET surface area for commercial TiO<sub>2</sub> was only 4 m<sup>2</sup>/g. Higher surface area and porous nanosheet structure of Pt/P-TiO<sub>2</sub> were beneficial for the exposure of catalytic sites on the surface of Pt/P-TiO<sub>2</sub> to interact with the reactants, and thus improved the catalytic activity of the synthesized Pt/P-TiO<sub>2</sub> to some extents.

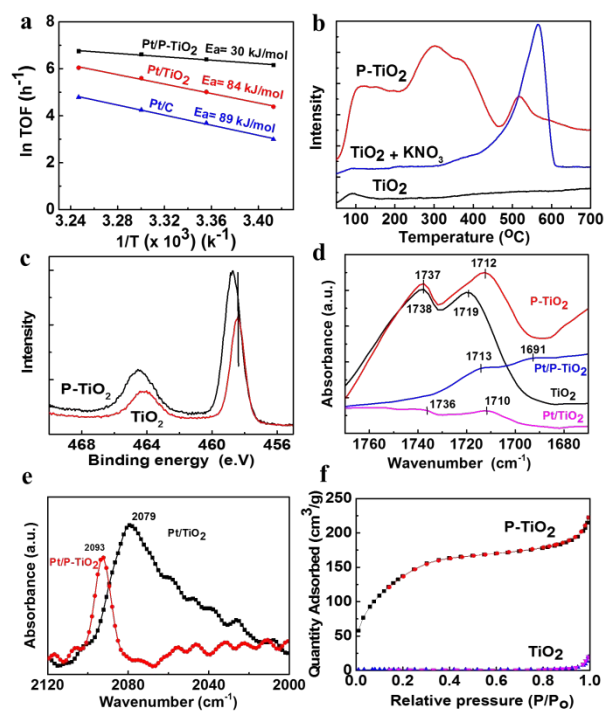


**Figure 2.** The natural logarithm of TOF (based on the total Pt amount) versus inverted temperature for apparent activation energy (a),  $\text{NH}_3$ -TPD of P-TiO<sub>2</sub>, commercial TiO<sub>2</sub> and the commercial TiO<sub>2</sub> mixed with about 2 wt% KNO<sub>3</sub> (b), XPS spectra of Ti 2p (c), *in situ* DRIFT spectra of acetone adsorbed on P-TiO<sub>2</sub>, TiO<sub>2</sub>, Pt/P-TiO<sub>2</sub> and Pt/TiO<sub>2</sub> (d), *in situ* DRIFT spectra of CO adsorbed on Pt/P-TiO<sub>2</sub> and Pt/TiO<sub>2</sub> (e), and N<sub>2</sub> adsorption-desorption isotherm of P-TiO<sub>2</sub> and TiO<sub>2</sub> (f).

## CONCLUSION

In conclusion, functional porous TiO<sub>2</sub> nanosheets supported Pt nanoparticles catalyst Pt/P-TiO<sub>2</sub> was successfully prepared, which showed excellent performance for the reductive amination of LA and its esters to produce various *N*-substituted pyrrolidones at ambient reaction conditions. Meanwhile, *N*-alkyl-2-piperidinones and *N*-arylisindolinones could also be efficiently synthesized from reductive amination of 4-acetylbutyric acid, 2-acetylbenzoic acid and 2-carboxybenzaldehyde, respectively. The high activity of Pt/P-TiO<sub>2</sub> under ambient conditions resulted from the high acidity of P-TiO<sub>2</sub>, the lower electron density of Pt sites as well as the porous structure. This work opens the way for efficient reductive amination of LA and its esters under ambient conditions. We believe that the synthesized Pt/P-TiO<sub>2</sub> has great potential of application for producing *N*-substituted pyrrolidones sustainably from LA and its esters.

## EXPERIMENTAL SECTION

**The preparation of P-TiO<sub>2</sub>.** In a typical procedure, tetrabutyl titanate (6 mmol) was mixed with potassium nitrate (15 g) completely by ball milling. The solid was further dried at 80 °C for 12 h to vaporize the generated *n*-butyl alcohol. After that, the obtained solid was calcined in air at 350 °C for 2 h. Finally, the product (P-TiO<sub>2</sub>) was achieved after being washed with

hot deionized water to remove KNO<sub>3</sub> and dried at 80 °C for 12 h under vacuum.

**The preparation of Pt/P-TiO<sub>2</sub>, Pt/TiO<sub>2</sub> and Pt/P25.** In a typical procedure for preparing Pt/P-TiO<sub>2</sub> (Pt 2 wt%), Pt/TiO<sub>2</sub> (Pt 2 wt%) and Pt/P25 (Pt 2 wt%), the prepared P-TiO<sub>2</sub> (0.2 g) or commercial TiO<sub>2</sub> or P25 (0.2 g) was initially dispersed into 50 mL aqueous solution of H<sub>2</sub>PtCl<sub>6</sub> (2 wt%) with stirring and kept overnight. Then, the H<sub>2</sub>PtCl<sub>6</sub> was reduced by NaBH<sub>4</sub> in ice-water bath. Subsequently, the solid was collected by filtration and washed by water and ethanol three times. Finally, the obtained powder was further dried at 80 °C for 12 h under vacuum. The contents of Pt in these three prepared catalysts were determined by ICP-AES (VISTA-MPX).

**Characterization.** The scanning electron microscopy (SEM) measurements were performed on a Hitachi S-4800 scanning electron microscope operated at 15 kV. The transmission electron microscopy (TEM) images were obtained using a TEM JEOL-1011 and TEM JEOL-2100F. Powder X-ray diffraction (XRD) patterns were collected on a Rigaku D/max-2500 X-ray diffractometer using Cu K $\alpha$  radiation ( $\lambda = 0.154$  nm). The N<sub>2</sub> adsorption-desorption isotherm was determined using the Micromeritics ASAP 2020M system. X-ray photoelectron spectroscopy (XPS) measurements were carried out on a ESCAL Lab 220i-XL spectrometer. The content of Pt in the Pt-Ti was determined by inductively coupled plasma atomic emission spectroscopy (ICP-AES VISTA-MPX).  $\text{NH}_3$ -TPD and CO-pulse titration were performed on Micromeritics' AutoChem 2950 HP Chemisorption Analyzer. CO-DRIFT spectra were collected on Bruker Tensor II spectroscope equipped with a MCT detector. The sample was prereduced at 300 °C for 2h and then cooled to 25 °C in a He flow (10 mL min<sup>-1</sup>). Taking this as the background, the sample was exposed to a 0.4% CO/He flow, and then purged in a He flow (10 mL min<sup>-1</sup>) to remove physically adsorbed CO. IR spectra of chemisorbed CO were recorded at 25 °C. Acetone-DRIFT spectra were collected on Bruker Tensor 27 spectroscope with a MCT detector. The sample was pressed into a self-supporting wafer and mounted into the quartz IR cell connected to a conventional flow system. The sample was prereduced at 300 °C for 2h and then cooled to 40 °C in a He flow (10 mL min<sup>-1</sup>). Taking this as the background, the acetone was bubbled into the IR cell by He flow and then purged in a He flow (10 mL min<sup>-1</sup>) to remove physically adsorbed acetone. IR spectra of chemisorbed acetone were recorded at 40 °C.

**Typical procedures for the reductive amination of LA.** In a typical experiment, desired amounts of substrates, catalysts and 2 mL methanol were charged into a glass bottle (10 ml) equipped with a magnetic stirrer. After sealing, the H<sub>2</sub> (in a balloon) was charged into the reactor. The reactor was then put into a water bath of 25 °C and the magnetic stirrer was started. After a certain reaction time, the hydrogen balloon was removed, and internal standard *n*-hexyl alcohol was added into the reactor. The reaction mixture was then analyzed quantitatively by GC (Agilent 6820) equipped with a flame-ionized detector and identification of the products was done by GC-MS (Shimadzu QP2010). To obtain the pure products, the reaction mixture was concentrated and purified by column chromatography (silica gel with petroleum ether/EtOAc). Meanwhile, the pure products were characterized by <sup>1</sup>H NMR, <sup>13</sup>C NMR, and HRMS, which were provided in detail in the Supporting Information.

**Reusability of the Pt/P-TiO<sub>2</sub>.** To examine the reusability of the Pt/P-TiO<sub>2</sub>, the catalyst was recovered by centrifugation and washed with methanol and ethyl ether (5 × 5 mL). After drying under vacuum at 80 °C for 12 h, the recovered catalyst was reused for the next run.

## ASSOCIATED CONTENT

### Supporting Information

The Supporting Information is available free of charge on the ACS Publications website.

The used materials, size distribution of Pt in the prepared Pt/P-TiO<sub>2</sub>, CO-pulse titration results of the used Pt catalysts, time-yield plots for the reductive amination of LA with *n*-octylamine, activity of different catalysts, solvent effect, reusability of the Pt/P-TiO<sub>2</sub>, TEM image and XPS spectra of the recovered catalyst, GC-MS spectra of the generated intermediate from butyl levulinate and *n*-octylamine, GC-MS spectra of the intermediate generated from LA and *n*-octylamine, <sup>1</sup>H NMR and <sup>13</sup>C NMR of the intermediate butyl 4-(phenylamino)pentanoate, effect of different additive on the catalytic activity of different catalysts, and the <sup>1</sup>H NMR, <sup>13</sup>C NMR, and HRMS data for all synthesized products.

## AUTHOR INFORMATION

### Corresponding Author

\*songjl@iccas.ac.cn

\*hanbx@iccas.ac.cn

### Notes

The authors declare no competing financial interests.

## ACKNOWLEDGMENT

This work was supported by National Natural Science Foundation of China (21673249, 21733011), the National Key Research and Development Program of China (2017YFA0403003), Beijing Municipal Science & Technology Commission (Z181100004218004), Key Research Program of Frontier Sciences of CAS (QYZDY-SSW-SLH013), and Youth Innovation Promotion Association of CAS (2017043).

## REFERENCES

(1) (a) Meng, Q.; Hou, M.; Liu, H.; Song, J.; Han, B. Synthesis of ketones from biomass-derived feedstock. *Nat. Commun.* **2017**, *8*, 14190. (b) Liang, G.; Wang, A.; Li, L.; Xu, G.; Yan, N.; Zhang, T. Production of primary amines by reductive amination of biomass-derived aldehydes/ketones. *Angew. Chem. Int. Ed.* **2017**, *56*, 3050-3054. (c) Zeng, H.; Cao, D.; Qiu, Z.; Li, C.-J. Palladium-catalyzed formal cross-coupling of diaryl ethers with amines: Slicing the 4-O-5 linkage in lignin models. *Angew. Chem. Int. Ed.* **2018**, *57*, 3752-3757. (d) Upton, B. M.; Kasko, A. M. Strategies for the conversion of lignin to high-value polymeric materials: Review and perspective. *Chem. Rev.* **2016**, *116*, 2275-2306. (e) Schutyser, W.; Renders, T.; Van den Bosch, S.; Koelewijn, S.-F.; Beckham, G. T.; Sels, B. F. Chemicals from lignin: an interplay of lignocellulose fractionation, depolymerisation, and upgrading. *Chem. Soc. Rev.* **2018**, *47*, 852-908. (f) Xia, Q.; Chen, Z.; Shao, Y.; Gong, X.; Wang, H.; Liu, X.; Parker, S. F.; Han, X.; Yang, S.; Wang, Y. Direct hydrodeoxygenation of raw woody biomass into liquid alkanes. *Nat. Commun.* **2016**, *7*, 11162. (g) Deng, W.; Wang, Y.; Zhang, S.; Gupta, K. M.; Hülsey, M. J.; Asakura, H.; Liu, L.; Han, Y.; Karp, E. M.; Beckham, G. T.; Dyson, P. J.; Jiang, J.; Tanaka, T.; Wang, Y.; Yan, N. Catalytic amino acid production from biomass-derived intermediates. *Proc. Natl. Acad. Sci. U. S. A.* **2018**, *115*, 5093-5098. (h) Hülsey, M. J.; Yang, H.; Yan, N.

Sustainable routes for the synthesis of renewable heteroatom-containing chemicals. *ACS Sustainable Chem. Eng.* **2018**, *6*, 5694-5707.

(2) (a) Serrano-Ruiz, J. C.; Luque, R.; Sepúlveda-Escribano, A. Transformations of biomass-derived platform molecules: from high added-value chemicals to fuels via aqueous-phase processing. *Chem. Soc. Rev.* **2011**, *40*, 5266-5281. (b) Zhang, Z.; Huber, G. W. Catalytic oxidation of carbohydrates into organic acids and furan chemicals. *Chem. Soc. Rev.* **2018**, *47*, 1351-1390. (c) Mika, L. T.; Cséfalvay, E.; Németh, Á. Catalytic conversion of carbohydrates to initial platform chemicals: Chemistry and sustainability. *Chem. Rev.* **2018**, *118*, 505-613. (d) Luo, W.; Sankar, M.; Beale, A. M.; He, Q.; Kiely, C. J.; Bruijninx, P. C. A.; Weckhuysen, B. M. High performing and stable supported nano-alloys for the catalytic hydrogenation of levulinic acid to  $\gamma$ -valerolactone. *Nat. Commun.* **2015**, *6*, 6540.

(3) (a) Vidal, J. D.; Climent, M. J.; Concepcion, P.; Corma, A.; Iborra, S.; Sabater, M. J. Chemicals from biomass: Chemoselective reductive amination of ethyl levulinate with amines. *ACS Catal.* **2015**, *5*, 5812-5821. (b) Touchy, A. S.; Siddiki, S. M. A. H.; Kon, K.; Shimizu, K. *ACS Catal.* **2014**, *4*, 3045-3050. (c) Wu, C.; Zhang, H.; Yu, B.; Chen, Y.; Ke, Z.; Guo, S.; Liu, Z. Lactate-based ionic liquid catalyzed reductive amination/cyclization of keto acids under mild conditions: A metal-free route to synthesize lactams. *ACS Catal.* **2017**, *7*, 7772-7776. (d) Siddiki, S. M. A. H.; Touchy, A. S.; Bhosale, A.; Toyao, T.; Mahara, Y.; Ohyama, J.; Satsuma, A.; Shimizu, K. Direct synthesis of lactams from keto acids, nitriles, and H<sub>2</sub> by heterogeneous Pt catalysts. *ChemCatChem* **2018**, *10*, 789-795. (e) Vidal, J. D.; Climent, M. J.; Corma, A.; Concepcion, D. P.; Iborra, S. One-pot selective catalytic synthesis of pyrrolidone derivatives from ethyl levulinate and nitro compounds. *ChemSusChem* **2017**, *10*, 119-128.

(4) (a) Das, S.; Addis, D.; Knöpke, L. R.; Bentrup, U.; Junge, K.; Brückner, A.; Beller, M. Selective catalytic monoreduction of phthalimides and imidazolidine-2,4-diones. *Angew. Chem. Int. Ed.* **2011**, *50*, 9180-9184. (b) Du, X.-L.; He, L.; Zhao, S.; Liu, Y.-M.; Cao, Y.; He, H.-Y.; Fan, K.-N. Hydrogen-independent reductive transformation of carbohydrate biomass into  $\gamma$ -valerolactone and pyrrolidone derivatives with supported gold catalysts. *Angew. Chem. Int. Ed.* **2011**, *50*, 7815-7819. (c) Ogiwara, Y.; Uchiyama, T.; Sakai, N. Reductive amination/cyclization of keto acids using a hydrosilane for selective production of lactams versus cyclic amines by switching of the indium catalyst. *Angew. Chem. Int. Ed.* **2016**, *55*, 1864-1867.

(5) (a) Wu, C.; Luo, X.; Zhang, H.; Liu, X.; Ji, G.; Liu, Z.; Liu, Z. Reductive amination/cyclization of levulinic acid to pyrrolidones versus pyrrolidines by switching the catalyst from AlCl<sub>3</sub> to RuCl<sub>3</sub> under mild conditions. *Green Chem.* **2017**, *19*, 3525-3529. (b) Wei, Y.; Wang, C.; Jiang, X.; Xue, D.; Li, J.; Xiao, J. Highly efficient transformation of levulinic acid into pyrrolidinones by iridium catalyzed transfer hydrogenation. *Chem. Commun.* **2013**, *49*, 5408-5410. (c) Wei, Y.; Wang, C.; Jiang, X.; Xue, D.; Liu, Z.-T.; Xiao, J. Catalyst-free transformation of levulinic acid into pyrrolidinones with formic acid. *Green Chem.* **2014**, *16*, 1093-1096.

(6) (a) Manzer, L. E.; Herkes, F. E. Production of 5-methyl-1-hydrocarbyl-2-pyrrolidone by reductive amination of levulinic acid. U.S. Patent 2004/0192933A1, **2004**. (b) Manzer, L. E. Production of 5-methyl-N-aryl-2-pyrrolidone and 5-methyl-N-cycloalkyl-2-pyrrolidone by reductive amination of levulinic acid with aryl amines. U.S. Patent 6743819 B1, **2004**. (c) Zhang, J.; Xie, B.; Wang, L.; Yi, X.; Wang, C.; Wang, G.; Dai, Z.; Zheng, A.; Xiao, F.-S. Zirconium oxide supported palladium nanoparticles as a highly efficient catalyst in the hydrogenation-amination of levulinic acid to pyrrolidones. *ChemCatChem* **2017**, *9*, 2661-2667. (d) Gao, G.; Sun, P.; Li, Y.; Wang, F.; Zhao, Z.; Qin, Y.; Li, F. Highly stable porous-carbon-coated Ni catalysts for the reductive amination of levulinic acid via an unconventional pathway. *ACS Catal.* **2017**, *7*, 4927-4935.

(7) (a) Huang, Y.-B.; Dai, J.-J.; Deng, X.-J.; Qu, Y.-C.; Guo, Q.-X.; Fu, Y. Ruthenium-catalyzed conversion of levulinic acid to pyrrolidines by reductive amination. *ChemSusChem* **2011**, *4*, 1578-1581. (b) Wang, S.; Huang, H.; Bruneau, C.; Fischmeister, C. Selective and efficient iridium catalyst for the reductive amination of levulinic acid into pyrrolidones. *ChemSusChem* **2017**, *10*, 4150-4154.

(8) (a) Murata, K.; Mahara, Y.; Ohyama, J.; Yamamoto, Y.; Arai, S.; Satsuma, A. The metal-support interaction concerning the particle size effect of Pd/Al<sub>2</sub>O<sub>3</sub> on methane combustion. *Angew. Chem. Int. Ed.* **2017**, *56*, 15993-15997. (b) Komanoya, T.; Kinemura, T.; Kita, Y.; Kamata, K.; Hara, M. Electronic effect of ruthenium nanoparticles on efficient

reductive amination of carbonyl compounds. *J. Am. Chem. Soc.* **2017**, *139*, 11493-11499.

(9) Song, S.; Wang, Y.; Yan, N. A remarkable solvent effect on reductive amination of ketones. *Mol. Catal.* **2018**, *454*, 87-93.

(10) (a) Wan, H.; Vitter, A.; Chaudhari, R. V.; Subramaniam, B. Kinetic investigations of unusual solvent effects during Ru/C catalyzed hydrogenation of model oxygenates. *J. Catal.* **2014**, *309*, 174-184. (b) Dong, B.; Guo, X.; Zhang, B.; Chen, X.; Guan, J.; Qi, Y.; Han, S.; Mu, X. Heterogeneous Ru-based catalysts for one-pot synthesis of primary amines from aldehydes and ammonia. *Catalysts* **2015**, *5*, 2258-2270.

(11) (a) Zhang, J.; Li, C.; Chen, X.; Guan, W.; Liang, C. Insights into the reaction pathway of hydrodeoxygenation of dibenzofuran over MgO supported noble-metals catalysts. *Catal. Today* **2019**, *319*, 155-163. (b) He, J.; Lu, L.; Zhao, C.; Mei, D.; Lercher, J. A. Mechanisms of catalytic cleavage of benzyl phenyl ether in aqueous and apolar phases. *J. Catal.* **2014**, *311*, 41-51. (c) Wang, L.; Wan, H.; Jin, S.; Chen, X.; Li, C.; Liang, C. Hydrodeoxygenation of dibenzofuran over SiO<sub>2</sub>, Al<sub>2</sub>O<sub>3</sub>/SiO<sub>2</sub> and ZrO<sub>2</sub>/SiO<sub>2</sub> supported Pt catalysts. *Catal. Sci. Technol.* **2015**, *5*, 465-474.

(12) Watanabe, S.; Ma, X.; Song, C. Characterization of structural and surface properties of nanocrystalline TiO<sub>2</sub>-CeO<sub>2</sub> mixed oxides by XRD, XPS, TPR, and TPD. *J. Phys. Chem. C* **2009**, *113*, 14249-14257.

(13) Song, J.; Zhou, B.; Zhou, H.; Wu, L.; Meng, Q.; Liu, Z.; Han, B. Porous zirconium-phytic acid hybrid: a highly efficient catalyst for Meerwein-Ponndorf-Verley reductions. *Angew. Chem. Int. Ed.* **2015**, *54*, 9399-9403.

(14) (a) Tang, H.; Wei, J.; Liu, F.; Qiao, B.; Pan, X.; Li, L.; Liu, J.; Wang, J.; Zhang, T. Strong metal-support interactions between gold nanoparticles and nonoxides. *J. Am. Chem. Soc.* **2016**, *138*, 56-59. (b) Tang, H.; Su, Y.; Zhang, B.; Lee, A. F.; Isaacs, M. A.; Wilson, K.; Li, L.; Ren, Y.; Huang, J.; Haruta, M.; Qiao, B.; Liu, X.; Jin, C.; Su, D.; Wang, J.; Zhang, T. Classical strong metal-support interactions between gold nanoparticles and titanium dioxide. *Sci. Adv.* **2017**, *3*, e1700231. (c) Zhao, H.; Yao, S.; Zhang, M.; Huang, F.; Fan, Q.; Zhang, S.; Liu, H.; Ma, D.; Gao, C. Ultra-small platinum nanoparticles encapsulated in sub-50 nm hollow titania nanospheres for low-temperature water-gas shift reaction. *ACS Appl. Mater. Interfaces* **2018**, *10*, 36954-36960.

(15) (a) Robinson, A. M.; Mark, L.; Rasmussen, M. J.; Hensley, J. E.; Medlin, J. W. Surface chemistry of aromatic reactants on Pt- and Mo-modified Pt catalysts. *J. Phys. Chem. C* **2016**, *120*, 26824-26833. (b) Sica, A. M.; Baibich, I. M.; Gigola, C. E. Preparation and characterization of alumina supported Pd-W and Pd-Mo catalysts photogenerated from group VI metal carbonyls. *J. Mol. Catal. A: Chem.* **2003**, *195*, 225-233. (c) Zafeiratos, S.; Papakonstantinou, G.; Jaksic, M. M.; Neophytides, S. G. The effect of Mo oxides and TiO<sub>2</sub> support on the chemisorption features of linearly adsorbed CO on Pt crystallites: an infrared and photoelectron spectroscopy study. *J. Catal.* **2005**, *232*, 127-136.

(16) (a) Brosius, R.; Kooyman, P. J.; Fletcher, J. C. Q. Selective formation of linear alkanes from n-hexadecane primary hydrocracking in shape-selective MFI zeolites by competitive adsorption of water. *ACS Catal.* **2016**, *6*, 7710-7715. (b) Fan, H.; Wang, Q.; Guo, J.; Jiang, T.; Zhang, Z.; Yang, G.; Han, B. Elimination of the negative effect of nitrogen compounds by CO<sub>2</sub>-water in the hydrocracking of anthracene. *Green Chem.* **2012**, *14*, 1854-1858. (c) Kwak, C.; Lee, J. J.; Bae, J. S.; Moon, S. H. Poisoning effect of nitrogen compounds on the performance of CoMoS/Al<sub>2</sub>O<sub>3</sub> catalyst in the hydrodesulfurization of dibenzothiophene, 4-methylthiophene, and 4,6-dimethylthiophene. *Appl. Catal. B-Environ.* **2001**, *35*, 59-68. (d) Hegedűs, L.; Szőke-Molnár, K.; Sajó, I. E.; Srankó, D. F.; Schay, Z. Poisoning and reuse of supported precious metal catalysts in the hydrogenation of N-heterocycles part I: Ruthenium-catalysed hydrogenation of 1-methylpyrrole. *Catal. Lett.* **2018**, *148*, 1939-1950. (d) Hegedűs, L.; Máthé, T. Hydrogenation of pyrrole derivatives: Part V. Poisoning effect of nitrogen on precious metal on carbon catalysts. *Appl. Catal. A-Gen.* **2002**, *226*, 319-322.

**For Table of Contents Use Only**